ISBN: 978-3-95450-241-7 ISSN: 2673-5350 doi:10.18429/JACoW-IBIC2022-WEP22

EXPERIMENTAL INVESTIGATION OF GOLD COATED TUNGSTEN WIRES EMISSIVITY FOR APPLICATIONS IN PARTICLE ACCELERATORS

A. Navarro*, M. Martin, F. Roncarolo, CERN, Geneva, Switzerland

Abstract

The operation of wire grids and wire scanners as beam profile monitors can be heavily affected, both in terms of measurement accuracy and wire integrity, by the thermal response of the wires to the energy deposited by the charged particles. Accurate measurements of material emissivity are crucial, as Radiative Cooling represent the most relevant cooling process. In this work, we present a method for emissivity measurements of gold-coated tungsten wires based on calorimetric techniques. The dedicated electrical setup allowed allowed transient and steady state measurements for temperatures up to 2000 K. A theoretical description of the measurement technique will be followed up by the electrical set up description and a detailed discussion about the measured results and uncertainties.

INTRODUCTION

Wire grids are examples of thin target detectors extensively used in particle accelerators for transverse beam profile measurements [1]. Depending on the the detector characteristics and beam parameters (intensity, energy, transverse and longitudinal beam size) the operation of the monitor can result in thermo-mechanical stresses, potentially perturbing the measurement accuracy and degrading the monitor integrity. To prevent these circumstances, a thorough understanding of the particle-detector interactions is of critical importance.

For simulating the particle-detector interaction and predict detector material heating and damage, a finite difference program has been implemented [2]. Uncertainties in the material properties such as melting (or sublimation) temperatures, heat capacity, thermal conductivity and/or emissivity, can induce large uncertainties in the simulation results. For published values in the scientific literature of the emissivity of tungsten wires (commonly used in particle accelerators), large uncertainties can be found. Figure 1 shows some examples of reported emissivity values as a function of the temperature.

To reduce the uncertainties of the thermal evolution models, we decided to experimentally measure the emissivity of gold-coated tungsten wires, widely used at CERN for wire grid detectors. Many techniques can be used for measuring the emissivity [3–5]. Each method has its own inherent advantages and drawbacks. The calorimetric method was used for the measurements reported in this paper. This methods gives information about the total hemispherical emissivity. The main advantage of this method is that it can measure small sample (~µm) sizes and it does not require expensive or sophisticated equipment. It is a direct absolute method, so no standard emissivity reference is necessary. Some disadvantages are: it is time consuming because it is typically performed in steady state; the sample needs to be placed under vacuum (typically 10^{-5} bar) to avoid convective losses; the measurement of the surface temperature is a big source of uncertainty.

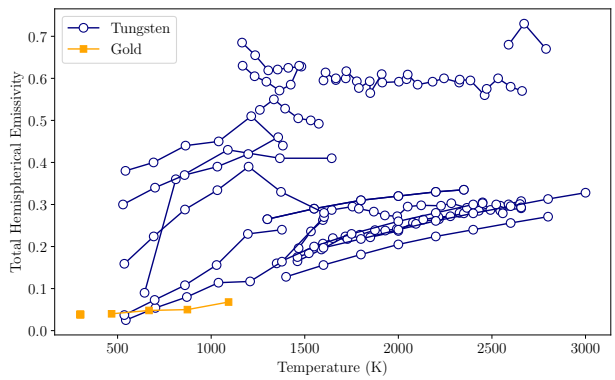

Figure 1: Examples of reported emissivity measurements for Gold and Tungsten. From Ref. [6].

SPECIFICS OF THE CALORIMETRIC METHOD

The calorimetric method is based on studying the energy balance of the sample material at a certain temperature, which is maintained via joule effect. For a temperature T, the resistance of a wire, with a wire length l(T), can be calculated by:

$$R(T) = \frac{\rho(T) l(T)}{S_f}, \quad (1)$$

where S_f is the section of the wire assumed to be constant over its length. $\rho(T)$ is the resistivity of the material and l(T) is the length of the sample, and they are both dependent on the material temperature. As a first approximation, l(T) can be modeled as a linear increase, $\Delta l(T) = l_0 \alpha_l (T - T_0)$, where α_l is the coefficient of thermal expansion. It is difficult to give a simple mathematical description of the variation of the resistivity with temperature, as it is very much material dependent. Tabulated values of the resistivity as a function of temperature can be found in literature.

Once thermal equilibrium is reached for a specific intensity, the average temperature of the sample can be determined by measuring the resistance and comparing it to the known values of R/R_0 for the material. The energy balance of the

* araceli.navarro.fernandez@cern.ch

ISBN: 978-3-95450-241-7 ISSN: 2673-5350 doi:10.18429/JACoW-IBIC2022-WEP22

system can be written as follows:

$$\left(\frac{\partial T}{\partial t}\right)_{tot} = \left(\frac{\partial T}{\partial t}\right)_{Ht} - \left(\frac{\partial T}{\partial t}\right)_{Rd} - \left(\frac{\partial T}{\partial t}\right)_{Con}, \quad (2)$$

where the term with the sub index Ht, represents heating, and it is accompanied by some cooling processes such as Radiative cooling (Rd) and Conduction cooling (Con). This term can be written as:

$$\left(\frac{\partial T}{\partial t}\right)_{Ht} = \frac{I^2 R(T)}{C_p(T)\rho_v V}. \quad (3)$$

Here I refers to the current applied to the wire sample and R is the resistance of that wire at a temperature T. C_p, ρ_v and V are the specific heat, the density and the volume of the wire. The heat power dissipated by radiation exchange between the surface (S) and the vacuum chamber at temperature T_0 is described by the Stefan-Boltzman law:

$$\left(\frac{\partial T}{\partial t}\right)_{Rd} = \frac{S\sigma_{SB}\epsilon(T)\left(T(x,t)^4 - T_0^4\right)}{C_p(T)\rho_v V}, \quad (4)$$

where σ_{SB} is the Stephan-Boltzmann constant and ϵ is the emissivity of the material. Finally, the thermal power loss due to thermal conduction can be described by Fourier's equation as follows:

$$\left(\frac{\partial T}{\partial t}\right)_{Con} = \alpha(T)\left(\frac{\partial^2 T}{\partial x^2}\right), \quad (5)$$

where $\alpha(T)$ is the so called thermal diffusivity of the medium (units of m^2/s).

In steady-state conditions ($\partial T/\partial t = 0$), Eq. (2) becomes a second order Boundary Value Problem (BVP) with Dirichlet boundary conditions (T(0) = T_{left} and T(L) = T_{right}). The solution of this equation can be calculated numerically. For that, the first step is to define a discrete set of nodes in the physical domain. Figure 2 shows an example of spatial discretization of an homogeneous wire. The parameter Δx indicates the local distance between the adjacent points in space.

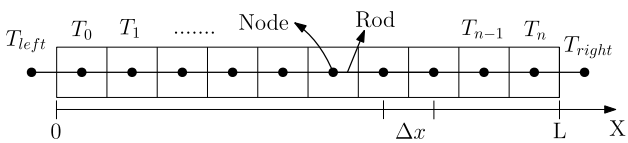

Figure 2: Space discretization of homogeneous rod.

Several numerical techniques exist to discretize the BVP [7]. For this study, a central difference (CD2) was considered for approximating the second order derivative. That is:

$$\left.\frac{d^2T}{dx^2}\right|_{x_i} = \frac{T_{i+1} - 2T_i + T_{i-1}}{2\delta_x^2} + O(\delta_x^2) \quad (6)$$

Note that with a little bit of algebra one can write the steady state equation as:

$$\begin{bmatrix} 1 & 0 & 0 & 0 & 0 & 0 \\ 1 & -2 & 1 & 0 & 0 & 0 \\ 0 & 1 & -2 & 1 & 0 & 0 \\ 0 & 0 & \ddots & \ddots & \ddots & 0 \\ 0 & 0 & 0 & 1 & -2 & 1 \\ 0 & 0 & 0 & 0 & 0 & 1 \end{bmatrix} \begin{bmatrix} T_0 \\ T1 \\ T2 \\ \vdots \\ T_N \\ T_{N+1} \end{bmatrix} = \begin{bmatrix} f_0 \\ f1 \\ f2 \\ \vdots \\ f_N \\ f_{N+1} \end{bmatrix},$$

where T_i are the unknowns of the BVP. $f_0 = T_{left}$ and $f_N = T_{right}$. While the rest can be written as:

$$f_i = \delta_x^2 \cdot \left(A + BT_i^4\right), \quad (7)$$

with $A = -\frac{1}{\alpha}\left(I^2R + S\epsilon\sigma_{SB}T_0^4\right)$ and $B = \frac{1}{\alpha}S\sigma_{SB}\epsilon$. Due to the T_i^4 term, this is nonlinear system of equations. For solving this system of equations Newton's method for non linear systems was used [7]. However, the objective of this study is to calculate the emissivity of the material, which is an extra unknown in our equation. For that, an iterative method with the following steps was used.

1. An initial guess of the emissivity is provided (ϵ_i^0, where the super-index indicates the iteration number).
2. With this value of the emissivity, the BVP is solved and then the average temperature along the wire is calculated (T_{sim}^n).
3. The numerically calculated average temperature is compared with the temperature measured experimentally (T_{meas}). The value of the emissivity is updated as follows:
$$\epsilon_j^{n+1} = \begin{cases} (\epsilon_j^n + 1)/2, & \text{if } e^n > 0 \\ (\epsilon_j^n)/2, & \text{if } e^n < 0 \end{cases}, \quad (8)$$
where $e^n = T_{sim}^n - T_{meas}$
4. This process is repeated until convergence.

EXPERIMENTAL DETAILS

A sketch of the experimental setup is shown in Fig. 3. The acquisition system consists of an assembly of two circuit boards: the measuring board and the acquisition board.

The measuring board has two main functionalities: holding the wire with both ends fixed on two turrets at a set distance, and measuring the current and the voltage drop in the wire. The current is measured by means of a shunt resistor, which was placed outside the vacuum to facilitate heat dissipation, and the voltage drop of the wire is measured directly at its mounting points, ensuring that only the voltage drop developed in the wire is taken into account. The board is located inside a vacuum vessel with a feed-through connector to transmit the signals across the vacuum barrier. The range of voltage (0 - 6 V) and intensity (0 - 2 A) applied to the wire cannot be directly measured by the Analogue-to-Digitcal Converters (ADC) and have to be processed beforehand by amplifiers with variable gain. The temperature at

ISBN: 978-3-95450-241-7 ISSN: 2673-5350 doi:10.18429/JACoW-IBIC2022-WEP22

the extremities of the wire (T_{left}, T_{right}) are measured by means of two temperature sensors mounted on the turrets.

The acquisition board captures and digitizes the measured signals, regulates the current flowing into the wire, and configures the measurement board for gain and common-mode offset. The measured current and voltage signals are digitized by the dual differential ADCs built into the microcontroller. The pulse conditioning block adapts the signal from the temperature sensors to the logic levels used by the microcontroller. The current, voltage and temperature signals are sent to a computer at a settable interval (minimum 100 µs) via a 1 Mbps USB serial connection.

The system is powered by a desktop power supply. Onboard DC-DC converters and linear regulators adapt the input voltage to the levels necessary to power the various analog parts of the circuit. The DAC, temperature sensor interface and the temperature sensors are powered by the USB connection from the computer. Four uncommitted amplifiers with BNC connectors are available to cross-check various signals with external equipment.

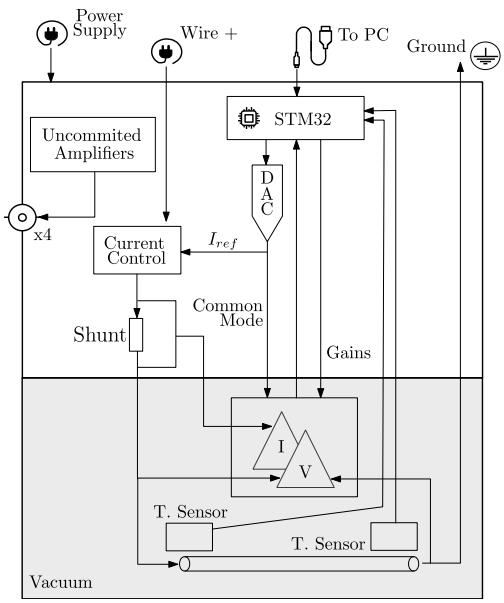

Figure 3: Schematic representation of electrical set-up.

RESULTS

For this analysis, Tungsten wires of two different diameters (20 µm and 40 µm) were measured, both with and without gold coating. Four samples of each wire type were measured to compile some statistics. Figure 4 shows the measured resistance (before calibration) as a function of time, for a 40 µm gold-coated Tungsten wire. In this case an intensity of 50 mA was provided. From this figure we can observe how the resistance increases until an equilibrium is reached. The steady-state (gray area) was considered to start when $dR/dt \lesssim 10^{-3}(\Omega/s)$. For each sample, the steady state resistance was computed for a variety of applied currents. A relationship between the average temperature and the applied intensity was calculated by comparing

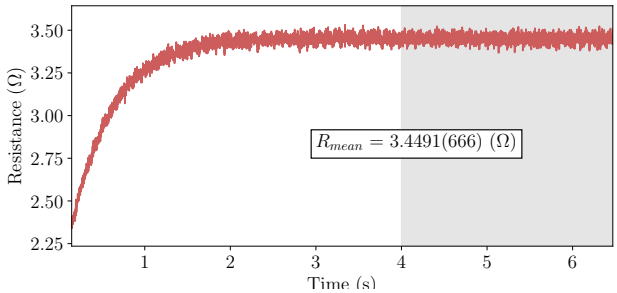

Figure 4: Raw data measurements (before calibration) of the resistance as a function of time. For a 40 µm gold-coated tungsten wire.

Table 1: Summary of R_0 Values for the Different Measured Cases

Composition	Diameter (µm)	R0 (ohm)
AuW	20	10.5(63)
AuW	40	1.438(76)
W	20	11.0(53)
W	40	1.562(58)

the measured resistance results with the tabulated values of R/R_0 [8]. To be able to compare our results to the tabulated ones, the value of R_0 was calculated using a parabolic model $R(I) = R_0 + AI^2$ and by extrapolating to zero. Only the low current ($I < 80$ mA) measurements were considered for determining R_0. Table 1 shows the values of the measured R_0 for the different samples. Note that the relative error when calculating R_0 for the 40 µm wires was smaller than 7%. However, the relative error for the 20 µm wires borders the 60%.

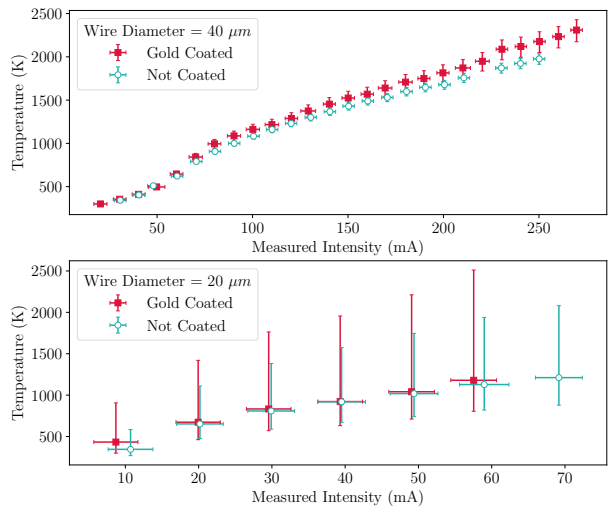

Figure 5: Mean temperature reached by the wires for different intensities. Top: 40 µm wires. Bottom: 20 µm wires.

The estimated values of the mean temperature as a function of the current are displayed in Fig. 5. A range of temperatures from 300 K to 2500 K was measured. The average temperature in the wires seemed to increase almost linearly

ISBN: 978-3-95450-241-7 ISSN: 2673-5350 doi:10.18429/JACoW-IBIC2022-WEP22

with the applied intensity. For the 20 µm wires, the uncertainties in the measurements of R_0 translated in big uncertainties in the determination of the wire temperature.

The boundary temperatures (T_{left} and T_{right}) increased quadratically with the applied current, always remaining below 350 K. Figure 6 shows the temperature (T_{left}) measured with the temperature sensors as a function of the applied intensity. For all the intensity range, $T_{left} \sim T_{right} \pm 1K$.

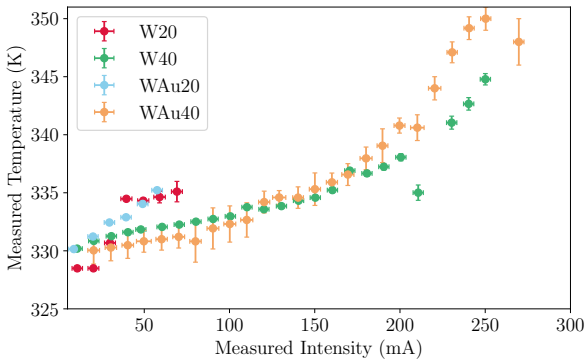

Figure 6: Summary of the boundary condition temperatures measured by the thermo-couple detectors at the extremes of the wires.

With increasing temperature, the temperature profile along the wire length becomes more constant. Figure 7 shows some examples of equilibrium thermal profiles computed for various currents. The numerical computation of the emissivity could be substantially simplified for high temperatures by assuming a constant profile. This is however not an accurate approximation at lower temperatures.

The emissivity of the material was calculated numerically for all the measured intensity range. It was not possible to determine the value of the emissivity for 20 µm wires due to the high uncertainties in the average temperature values. Figure 8 shows the computed values for the emissivity of the 40 µm wires. For both gold-coated and pure tungsten wires, the emissivity increased as the temperature increased. The emissivity of the pure tungsten wires was, in average, larger than the emissivity of the gold-coated tungsten wires, ranging from 0.087(12) up to 0.176(21). The emissivity values

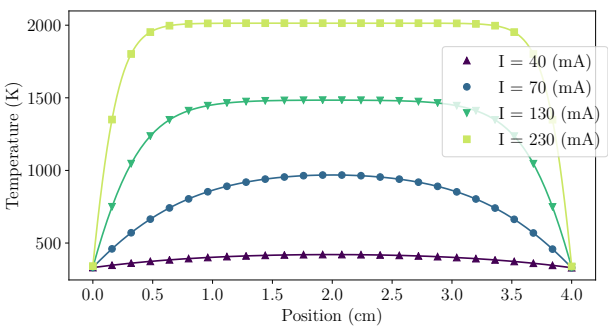

Figure 7: Steady state temperature profile calculated for different intensities.

for the gold-coated tungsten wires appear to be consistent with the reported values of the emissivity of gold. In the case of pure tungsten wires, both the slope of measured values agree with some published references. Particularly those reporting values of poor electromagnetic radiators. The average statistical relative error for the measured values (error bars in Fig. 8) was of 15.21% in the case of pure tungsten wires and 26.26% for gold-coated tungsten wires.

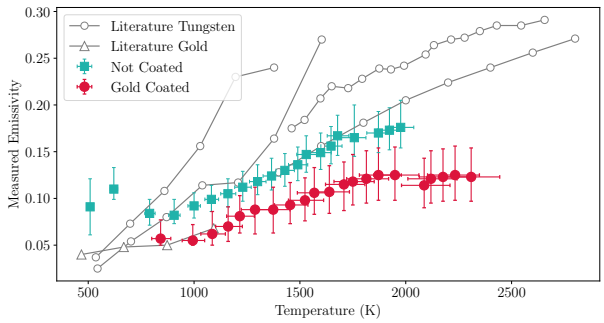

Figure 8: Emissivity of 40 µm. tungsten wires as a function of temperature.

CONCLUSIONS

In this article, a method to measure the emissivity of thin wires has been presented. Knowing accurately the value of the material is critical to properly simulate the thermal evolution of thin target detectors in particle accelerators. The measurement was done by means of the calorimetric methods. A dedicated set up, allowed for precise voltage and current measurements up to 2 A and 6 V respectively, which allowed for temperatures up to 2000 K to be measured. Due to the non-linearity of the BVP, numerical methods had to be used to determine the value of the emissivity. Several samples of tungsten wires (40 µm gold-coated and without coating) were measured. The values of the emissivity of the gold-coated wires appear to be consistent with the reported values of gold emissivity. The pure tungsten wires presented a systematically higher emissivity, however always smaller than 0.2. The average statistical error of the measured values was 15.21% for gold-coated wires and 26.26% for pure tungsten wires.

REFERENCES

[1] P. Forck, "Lecture notes on beam instrumentation and diagnostics", Joint Universities Accelerator School (JUAS 2010). http://www-bd.gsi.de

[2] A. Navarro Fernandez, F. Roncarolo and M. Sapinski, "Development of a Thermal Response Model for Wire Grid Profile Monitors and Benchmarking to CERN LINAC4 Experiments", in *Proc. IBIC'20*, Santos, Brazil, Sep. 2020, pp. 82–85. doi:10.18429/JACoW-IBIC2020-TUPP35

[3] A. El Bakali, R. Gilblas, T. Pottier, and Y. Le Maoult, "A fast and versatile method for spectral emissivity measurement at high temperatures", *Rev. Sci. Instrum.*, vol. 90, no. 11, p. 115116, 2019. doi:10.1063/1.5116425

[4] M. Honner and P. Honnerová, "Survey of emissivity measurement by radiometric methods", *Appl. Opt.*, vol. 54, no. 4, pp. 669-683, 2015. doi:10.1364/AO.54.000669

ISBN: 978-3-95450-241-7 ISSN: 2673-5350 doi:10.18429/JACoW-IBIC2022-WEP22

[5] C. Zhu, M. J. Hobbs and J. R. Willmott, "An accurate instrument for emissivity measurements by direct and indirect methods", *Meas. Sci. Technol.*, vol. 31, no. 4, p. 044007, 2020. doi:10.1088/1361-6501/ab5e9b

[6] Y. S. Touloukian, R. W. Powell, C. Y. Ho and P. G. Klemens, "Thermophysical properties of matter - the TPRC data series. Data book", United States, 1971.

[7] A. Meseguer, *Fundamentals of Numerical Mathematics for Physicists and Engineers*, Wiley, 2020.

[8] D. R. Lide, *CRC handbook of chemistry and physics*, vol. 85, CRC Press, 2004. doi:10.1201/9781315380476